

Sleep states alter ventral medullary surface responses to blood pressure challenges

D. M. RECTOR,¹ C. A. RICHARD,^{2,3} R. J. STABA,² AND R. M. HARPER²

²Department of Neurobiology and the Brain Research Institute, University of California at Los Angeles, Los Angeles, 90095-1763; ³Department of Neurology, University of California, Irvine Medical Center, Orange, California 92868; and ¹Biophysics Group, Los Alamos National Laboratory, Los Alamos, New Mexico 87545

Rector, D. M., C. A. Richard, R. J. Staba, and R. M. Harper. Sleep states alter ventral medullary surface responses to blood pressure challenges. *Am J Physiol Regulatory Integrative Comp Physiol* 278: R1090–R1098, 2000.—Ventral medullary surface (VMS) activity declines during rapid eye movement (REM) sleep, suggesting a potential for reduced VMS responsiveness to blood pressure challenges during that state. We measured VMS neural activity, assessed as changes in reflected 660-nm wavelength light, during pressor and depressor challenges within sleep/waking states in five adult, unrestrained, unanesthetized cats and in two control cats. Phenylephrine elevated blood pressure and elicited an initial VMS activity decline and a subsequent rise in VMS activity in all states, although the initial decline during quiet sleep occurred only in rostral placements. Phasic REM periods elicited a momentary recovery from the evoked activity rise, and arousals diminished the overall elevation in activity. A sodium nitroprusside depressor challenge increased VMS activity more in REM sleep than in quiet sleep, with the increase being even less in waking. Enhanced responses to depressor challenges during REM sleep suggest a loss of dampening of evoked activity during that state; state-related differential baroreflex sensitivity may result from sleep-waking changes in VMS responses to blood pressure challenges.

optical imaging; rapid eye movement sleep; quiet sleep; cat; baroreceptor reflex

THE RAPID EYE MOVEMENT (REM) sleep state exhibits significantly altered physiological characteristics from waking and quiet sleep (QS) states. These characteristics include widespread muscle atonia, greatly enhanced respiratory and heart rate variability, and a substantial redistribution of blood flow between splanchnic and skeletal beds (17). A loss of effectiveness of stimuli that normally elicit breathing or cardiovascular responses (25) and unresponsive physiological outcomes to forebrain thermal or electrical stimulation are also typical of REM sleep (5, 24). Despite this relative insensitivity to stimuli, REM sleep is also characterized by short bursts of motor activity and substantial cardiovascular and respiratory variation.

The costs of publication of this article were defrayed in part by the payment of page charges. The article must therefore be hereby marked "advertisement" in accordance with 18 U.S.C. Section 1734 solely to indicate this fact.

Regions within the ventral medullary surface (VMS) have the potential to modulate state-related reflex blood pressure challenges. A variety of stimulation, blockade, recording, and functional anatomic studies implicate neurons on or near the VMS in blood pressure regulation (7, 10, 15, 22; for review, see Ref. 4). The greatest proportion of data gathered on VMS contributions to breathing and blood pressure control has, however, been derived from anesthetized preparations or decerebrate preparations in which the effects of state have been eliminated. Those preparations were necessary because of the near-prohibitive logistic efforts required to place and maintain recording or stimulating electrodes on this ventral brain site in an intact preparation.

If contributions of anesthesia on "spontaneous" VMS activity are examined, remarkable differences emerge in neural responses to blood pressure or ventilatory challenges between waking and anesthetized states. Activity within the rostral VMS declines to a pressor challenge under either barbiturate anesthesia in the cat (10) or halothane anesthesia in the goat; but, in waking, modest activity increases occur. Depressor challenges administered during anesthesia, which activate rostral VMS activity, increase activity even more in waking (11). Comparable state effects on VMS activity also emerge with ventilatory challenges. A ventilatory hypercapnic challenge in goats, for example, elicits a substantial, short latency VMS activity increase, followed by a sustained decrease during waking conditions; but, that transient response is abolished under anesthesia, and the later decline is more modest (6). Sleep-waking differences in reflex responses to cardiovascular or respiratory stimuli are also evident in areas closely associated with the VMS; application of CO₂ to the underlying retrotrapezoid nucleus enhances breathing in the awake rat but that stimulation is ineffective in sleep (14).

The rostral VMS of the goat (27) and both rostral and intermediate VMS areas of the cat (29) show a substantial decline in spontaneous activity during REM sleep. The diminished VMS activity during REM sleep has the potential to modify the overall responsiveness of cells within this region to external input, compared with QS or waking. To examine this possibility, we measured VMS activity responses to transient hyper- and hypotension during waking, QS, and REM sleep

states in unanesthetized, freely moving cats with the use of optical procedures. Optical procedures allowed visualization of neural activity over relatively large VMS areas and provided an indication of regional patterns at relatively high temporal resolution. The procedure captures scattered and reflected light from local illumination at discrete wavelengths. Because cell discharge alters membrane properties, which in turn change light transmission and scattering, an indication of neural activation can be derived by capturing the reflected light (1). Illumination at long (red) or short (green) wavelengths allows differential assessment of activity and hemodynamic components, respectively, thus offering insights into the time course of neural and perfusion changes (8, 16).

Rostral and intermediate areas were targeted to compare with data previously collected in anesthetized animals and to provide supplemental information to waking and anesthesia findings from an earlier rostral VMS study in goats (11). New developments in imaging technology, including substantial miniaturization and enhanced sampling rates (28), allowed light reflectance measurement within the very small physical constraints of the cat VMS and with high spatial ($>7.0 \text{ mm}^2$) and temporal (50 Hz) resolution.

METHODS

Optical recording device. The imaging device (Fig. 1), described elsewhere (28), is a miniaturized version of a device used earlier for *in vivo* examination of neural activity in larger animals (27). We illuminated the VMS with light of two wavelengths, in the red ($660 \pm 10 \text{ nm}$; optimal for cell membrane displacement measures) and green ($560 \pm 10 \text{ nm}$; optimal for detection of perfusion changes) ranges. The procedure collects red scattered light from a depth of up to $500 \mu\text{m}$ (26) and green light from a depth of $250 \mu\text{m}$ (29).

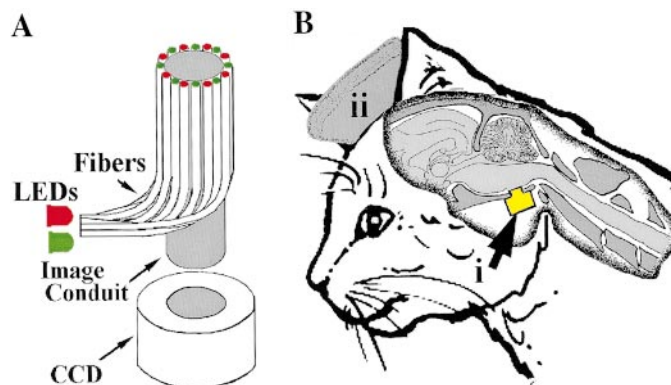


Fig. 1. Imaging device (A) consists of a charge-coupled device (CCD) with a 3.2-mm-diameter, 4.0-mm-long coherent image conduit attached directly to a CCD by optical epoxy. Tissue is illuminated by green (560 nm) and red (660 nm) light-emitting diodes (LEDs) that pass light through optic fibers on the circumference of the coherent optic conduit; green and red illumination are carried through alternating fibers. Electronics associated with the CCD and shaft of the imaging conduit are covered with black epoxy for light protection and for rendering the device impervious to fluids. Device is placed behind esophagus and trachea (B), with body of the CCD (i) resting on the ventral skull bone and the conduit penetrating the skull to the ventral medullary surface. Leads carry video and LED power signals under the skin to an epoxy headcap (ii).

Reflected and scattered light was passed through a 4.0-mm-long, 3.2-mm-diameter coherent image conduit made from 10,000 strands of $12\text{-}\mu\text{m}$ glass fibers with an attached 208×192 -pixel charge-coupled device (CCD; Texas Instruments TC211). Red and green light-emitting diodes provided illumination through flexible optic fibers attached around the probe perimeter; 30 fibers, those carrying red light alternating with those carrying green light, were illuminated using an external switching circuit.

A switching circuit alternated red and green illumination with light of each wavelength "on" for 7 ms and "off" for 3 ms during frame readout, for a duration of 10 ms/wavelength or 20 ms for both red and green wavelengths; i.e., 50 frames/s were collected from red and green illumination, respectively. Switching time was insignificant, there was no concurrent green and red illumination, and no illumination was delivered during image readout. The intensity of the light projected onto the VMS was monitored with a photodiode and servocontrolled to maintain a constant illumination level. To optimize the dynamic range for recording of light signals, illumination intensity was set so that maximal reflectance was two-thirds of the maximum digitizer value and the black level was set to half of the amplitude of the minimal pixel value. The imaging device measured $\sim 4.0 \times 4.0 \text{ mm}$, and thus could be placed within the neck tissue of a cat without affecting swallowing, chewing, or food passage.

Surgical procedures. Seven adult cats, 3–4 kg in weight, underwent a recovery surgical procedure. The animals were anesthetized with 25 mg/kg pentobarbital sodium, supplemented with 10 mg/kg as needed. Atropine was administered in conjunction with initial anesthesia (0.05 mg/kg). Under sterile conditions, two sets of Teflon-coated, multistranded, stainless steel wires were placed into the lateral costal diaphragm via a left abdominal incision to later assess electromyographic (EMG) and electrocardiographic (ECG) activity. Two screws in the posterior skull provided a ground reference, and two screws in the anterior skull were used to record electroencephalographic (EEG) signals. An additional screw was placed in the bone over the orbit to acquire eye movement signals, and multistranded wires were placed into the nuchal muscles to acquire indications of muscle tonus. Electrode leads were threaded under the skin to a headpiece connector. The carotid artery and jugular vein on one side were cannulated for subsequent arterial pressure monitoring and pharmacological delivery, respectively. With the cat in the supine position, the trachea, esophagus, and associated soft tissue were exposed with a midline incision. The soft tissues were separated to visualize the basal skull and foramen magnum. An opening was made in the bone over the ventral medulla 3.0 mm rostral to the foramen magnum and just medial to the right tympanic bulla. A portion of the bulla was removed to provide access for the imaging device.

The imaging device was positioned in contact with the dura over the VMS using a micromanipulator. Stainless steel screws were placed into the skull, and the camera and probe were sealed in place with dental acrylic that filled the entire opening required for initial placement. The sealed opening minimized brain movement associated with cardiac and respiration-related pressure changes. A small cable carried the camera signals and illumination power from the camera through the neck tissue to the head connector.

After surgery, the cats received a regimen of antibiotics (penicillin G, 10^6 U im daily) and medication for analgesia. Dexamethasone ($0.4 \text{ mg/kg iv daily}$, decreasing to $0.05 \text{ mg}\cdot\text{kg}^{-1}\cdot\text{day}^{-1}$) was administered to minimize brain edema.

Optical and electrophysiological acquisition procedures. Scanned CCD pixels were digitized with a resolution of 12 bits. Images were digitized continuously, alternating between red and green illumination throughout the waking and sleep states, together with the electrophysiological signals (1 kHz/channel).

The diaphragmatic EMG signal was full-wave rectified and smoothed with a moving-average digital filter. Physiological signals were band-pass filtered (EEG, 0.1–60 Hz; ECG, 1–100 Hz; EMG, 10 Hz–1 kHz; integrated diaphragm EMG, 0–30 Hz; blood pressure, 0–30 Hz; electrooculogram, 1–30 Hz) and amplified on a Grass 78 polygraph; the data were simultaneously written on paper and stored in multiplexed form, together with the image data, on digital media.

Experimental protocol. The animals were placed daily in a 1-m³ recording chamber with food, water, and bedding for 1–4 h beginning 1–2 days after surgery for acclimatization. Rectal temperature was measured daily. Ambient temperature was maintained at 20°C, and a light period was maintained between 0600 and 1800. Low-compliance tubing was attached to the arterial catheter for blood pressure monitoring, and electrodes were attached to the recording apparatus through a commutator. Electrode and vascular patency assessments were carried out in the chamber over the subsequent 4–7 days; however, no pharmacological interventions were made, and no data were collected during this initial acclimatization, because of potential confounding effects from adaptation and lingering anesthetic effects. After the initial adaptation period, animals were recorded on a near-daily basis over a period of 3–9 wk (the prolonged period was required because multiple challenges were required for each state and only 1 challenge could be delivered for any 1 state). Because normal sleep was required for the studies, data were collected during daytime recordings, because the cats preferentially slept during that time. The recording protocol for each day began with an uninterrupted, complete waking/quiet sleep/active sleep cycle to establish baseline levels. Blood pressure challenges were delivered during one state in the subsequent sleep cycle, i.e., during waking, quiet sleep, or REM sleep, with the order of state administration determined randomly. Additional sleep cycles were then obtained, and blood pressure challenges were delivered in the remaining states. Pressor and depressor challenges were administered through the venous cannula while the animal breathed room air. Pressor challenges consisted of 20 or 30 µg iv phenylephrine through an indwelling jugular vein catheter. Sodium nitroprusside was infused intravenously as a bolus of 30–40 µg, sufficient to lower blood pressure by 35–50% from baseline. Because each sleep cycle was typically followed by arousal, eating, grooming, and other behaviors, challenges were separated by 10–90 min; no new challenges were administered until all cardiorespiratory variables had returned to baseline. Waking periods were taken from epochs in which animals were alert, but exhibiting minimal movement. Challenges during REM were delivered immediately on recognition of physiological characteristics of that state. Recordings were taken continuously during the entire state sequences during which the pressor or depressor challenges were delivered (10–30 min).

Data analysis. The recordings were scored for sleep states using standard criteria adopted for the cat (31). Processing of the images, including subtraction of experimental from control frames, image averaging, gray scale and contrast correction, and display of resulting frames was performed on an Intel Pentium-based computer. Successive images from each state were used to derive an average image reflectance intensity for red and green illumination for that state. Red

illumination was used to assess cell swelling associated with discharge, and green illumination was used to assess hemodynamic changes. The average values for each illumination wavelength and state were plotted together with electrophysiological measurements during the entire recording, including epochs with pressor and depressor challenges. Difference images were also calculated by subtracting averaged images of the experimental challenge from the average of the preinjection baseline. The resulting difference images were pseudocolored to convey statistically significant change in activation such that yellow-to-red-to-white colors represent increased cellular activation (decreased reflectance) and blue-to-purple-to-black colors represent decreased cellular activation (increased reflectance). Green pixels represent no statistically significant change from baseline conditions ($P < 0.05$). The availability of two illumination wavelengths assisted in determination of movement artifacts, because signal components contributed by motion affect reflectance of both illumination wavelengths in the same manner. Averaging of the optical data allowed normalization to ensure against overrepresentation of values from any one animal or contributions from any one state. Recordings were extensive (near daily for 3–9 wk), with multiple collections of trials from each state condition. Recordings were continued until sufficient representation from each state was obtained, an advantage offered by the chronic optical procedure.

Images were collected continuously; those selected from the challenge condition began with the first inflection of blood pressure change (typically 2–3 s postpharmacological administration) and were compared with preinjection baseline values. ANOVA procedures were used to detect differences in pixels between pressor or depressor and control conditions. Significance for differences in individual pixel values was assigned when $P < 0.05$.

Respiratory measures during both challenges were determined on a breath-by-breath basis from diaphragmatic inspiratory efforts. Total cycle times were calculated as intervals between the maximal values. Heart rate values were determined on a beat-by-beat basis using a peak-trough detection procedure. Because of non-normal variability in measures, Mann-Whitney (unpaired) and Wilcoxon (paired) nonparametric tests were used for overall physiological and activity assessment between states.

Probe localization assessment. After experiments were completed, the cats were euthanized with an overdose of pentobarbital sodium. The medullae were preserved with 10% phosphate-buffered formaldehyde and examined for localization of probe position.

RESULTS

Probe position. The location of probes for the experimental animals is outlined in Fig. 2. Control sites included positions in the pons and at the spinomedullary junction, just rostral to the first cervical nerve.

Arousal responses. Both pressor and depressor challenges often elicited arousal from sleep, as indicated by an increase in EEG frequency and restoration of nuchal tone. Arousals from sleep to waking from blood pressure challenges or other stimuli, such as noise, or “spontaneous” arousals resulted in decreased VMS activity (red reflectance increase). Perfusion also decreased (green reflectance increased) during such arousals. The arousal response confounded the “pure” response to the blood pressure challenge, because the arousal component could be additive or subtractive to

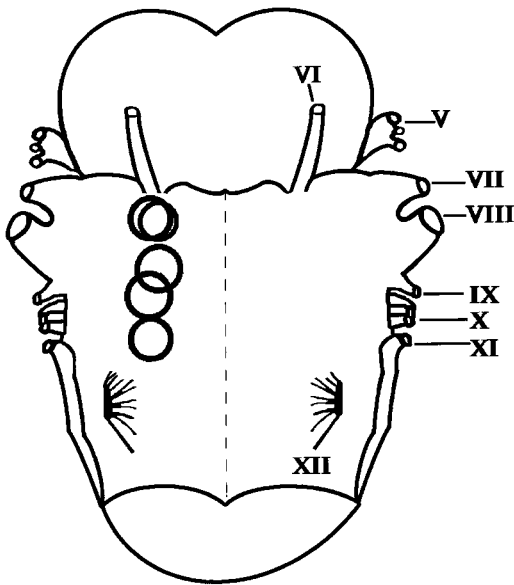


Fig. 2. Outline of probe placements for experimental animals on ventral medullary surface (VMS).

the blood pressure challenge effects. For this reason, responses to blood pressure challenges that did not result in arousal are presented to prevent confounding alerting influences.

Responses to pressor challenges. Phenylephrine administration increased blood pressure and decreased heart rate. During waking, VMS cells exhibited a biphasic response, with an initial decrease in activity (as indicated by increased red light reflectance), followed by an increase in activity (decreased reflectance; single subject in Fig. 3 and grouped data in Fig. 4). The nadir of the initial fall in activity during waking occurred with a latency of 19 s after injection and was significantly below baseline (Fig. 4, 4.5%; $P < 0.002$). The peak increase emerged at a latency of 51 s postinjection and was significantly above baseline (Fig. 4, ~6%;

$P < 0.001$). This increase lasted 190–200 s (Fig. 4). Phenylephrine administration during REM sleep also elicited an initial decline, followed by an increase; the magnitude of the response was slightly diminished over that of waking or QS when arousals during the challenge were excluded (Fig. 4). The nadir of the initial fall in activity during REM sleep was faster than that for waking, with a latency of 5–6 s, but an extent of decline equal to that for waking (–4.5%; $P =$ not significant). The peak of the subsequent rise in activity occurred with a latency of 57 s and an amplitude of 4.3% above baseline. VMS activity returned to baseline ~90 s after phenylephrine administration. Momentary phasic activity during REM sleep resulted in a transient biphasic activity response, with the second component moving toward baseline values; such an occurrence of a phasic event is shown in Fig. 3. During QS, only the more rostral sites elicited an initial decline; the remaining sites exhibited no initial activity loss, instead, activity increased rapidly after a longer latency (8–20 s). The maximum activity increase was 6.9% and lasted >200 s (Fig. 4).

Responses to depressor challenges. Nitroprusside, administered at levels that decreased blood pressure by 35–50% during waking conditions, increased VMS activity during all three states, although in the waking state the increase was preceded by a small decline (Fig. 5). The averaged increase in peak activity was significantly larger (15%) in REM sleep over waking (1.5%; $P < 0.02$) and QS (6.9%; $P < 0.03$) after removal of trials in which arousals occurred during the challenge (Fig. 6). The latency to the peak response was longer in REM sleep (59 s) than in QS (49 s; $P < 0.02$) or waking (38 s; $P < 0.03$). The latency to the nadir in the waking response was 71 s. It is noteworthy that, for the waking responses to nitroprusside, partitioning the data into rostral sites and nonrostral sites produced a much more pronounced rise in activity for the nonrostral sites. The reflectance trace for perfusion grossly paralleled the

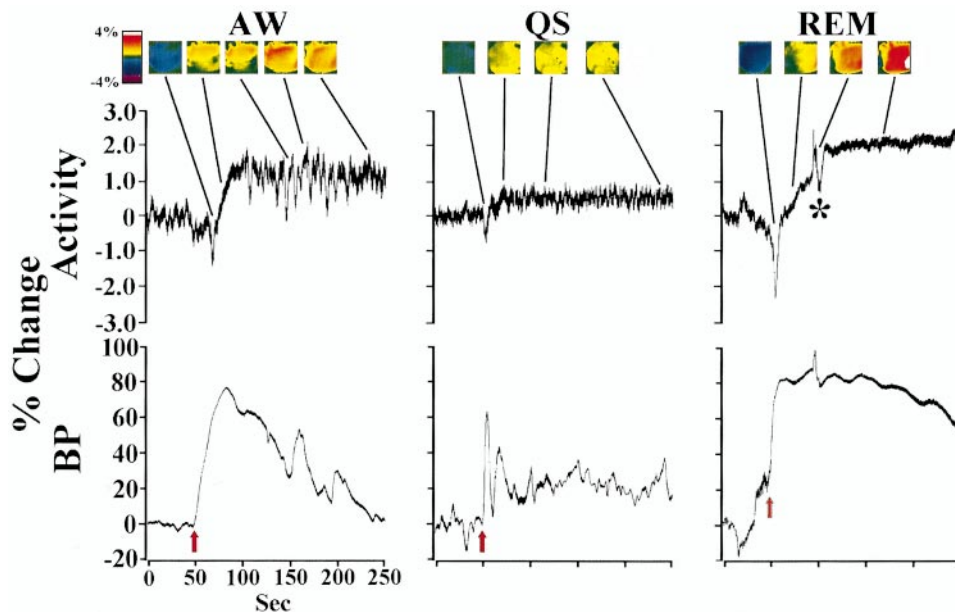


Fig. 3. Plots of individual activity traces (Activity) from a single cat and selected images, averaged across 3-s segments, together with associated blood pressure (BP) changes within waking (AW), quiet sleep (QS), and rapid eye movement (REM) sleep during a 30 μ g phenylephrine challenge. Arrows indicate onset of phenylephrine effects. Momentary biphasic optical pattern at asterisk (*) indicates a phasic REM epoch. Initial activity decline is coded as blue-purple as indicated by color scale, and later activity increase is coded as yellow-red-white.

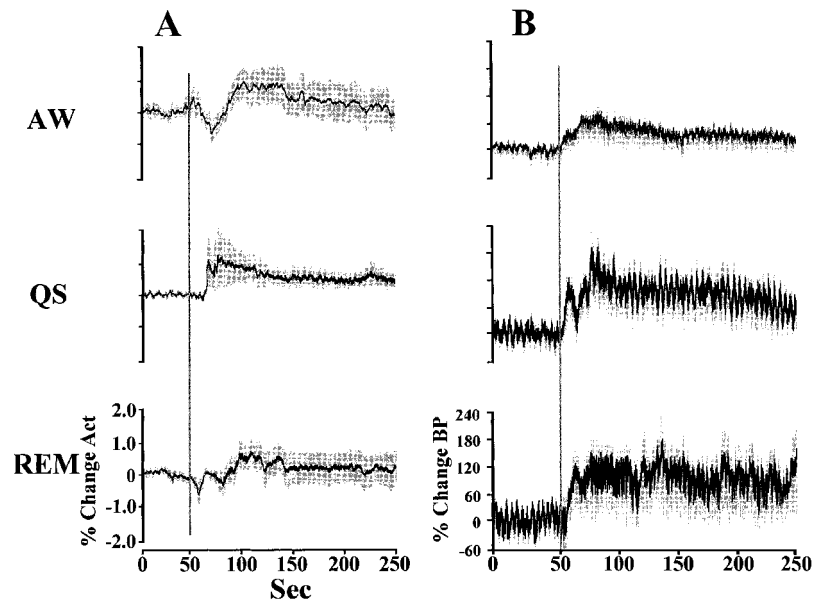


Fig. 4. Averaged traces of activity responses (A) and averaged blood pressure (B) together with SE (shading) within waking, QS, and REM sleep during phenylephrine challenges. Onset of blood pressure rise is indicated by vertical line.

values for activity. Nitroprusside also increased heart rate and respiratory rates during the challenge within waking or QS.

Control responses. Overall signal changes averaged from a control site, the spinomedullary junction, together with blood pressure changes during pressor and depressor challenges are shown in Fig. 7. Although blood pressure changes to the challenges were comparable to those encountered in the experimental preparations, the evoked neural activity changes were minimal, with differences of more than a factor of five in changes from VMS responses in REM sleep from those of the control site.

Topographic changes. The overall traces shown in Figs. 3–6 represent the summed changes with each challenge across the entire area under the probe; those

average responses were similar across the probe positions, except for the rostral-caudal QS response to phenylephrine and waking response to sodium nitroprusside described above. However, the sampled images of VMS regions shown in Figs. 3 and 5 indicate that isolated areas within the field of view can respond with little change, or with changes in the opposite direction to the overall trend. After a phenylephrine challenge (Fig. 3), regional changes are evident; after an initial decline in activity in waking, an activity rise occurs, principally apparent in the upper regions of the field of view. The response to a pressor challenge during REM sleep more markedly increases activity on the right side of the field of view in this subject. The initial overall increase in VMS activity with nitroprusside infusion, illustrated in the first waking response image

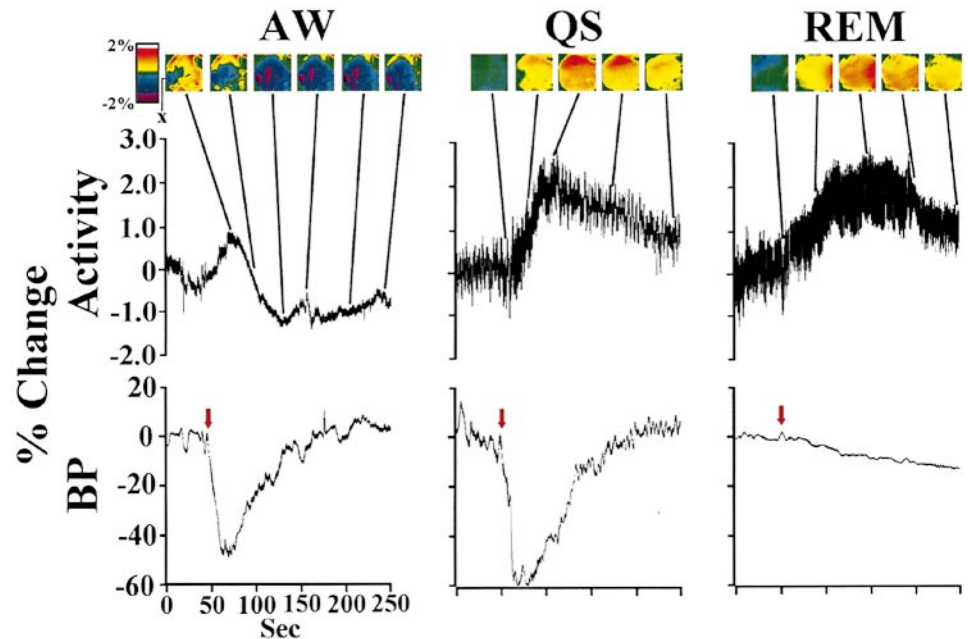


Fig. 5. Plots of individual activity traces (Activity) from a single cat and selected images, averaged across 3-s segments, together with associated BP changes within waking, QS, and REM sleep during a sodium nitroprusside challenge sufficient to lower blood pressure by 30–50% (onset of response at arrow). An early activation of the VMS occurs in waking; however, beginning of a decline is found within a midline region (indicated by "x"); that regional activity decline continues until nearly entire field of view is involved (coded as blue-purple).

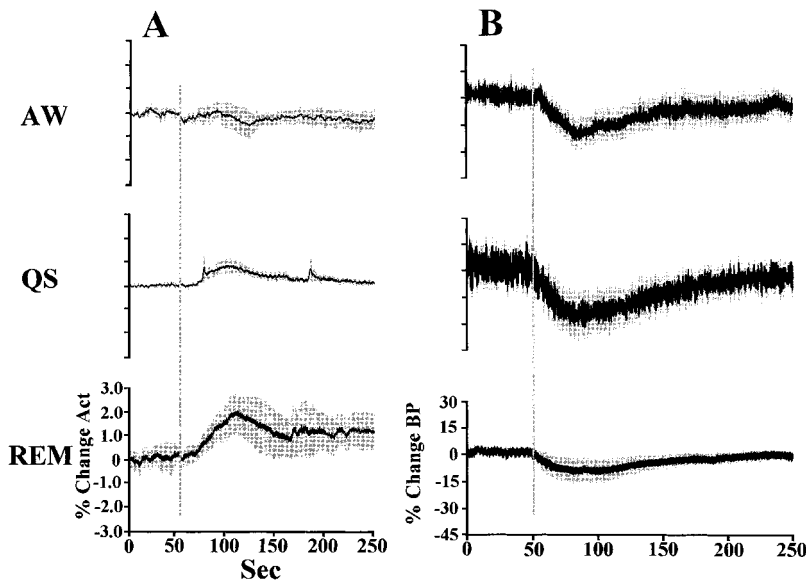


Fig. 6. Averaged traces of activity responses (A) and averaged BP (B) together with SE (shading) within waking, QS, and REM sleep during sodium nitroprusside challenges sufficient to lower blood pressure by 30–40% (onset of response at vertical line). Sharp deflections in activity trace for QS were associated with deep sighs in 1 cat.

in Fig. 5, indicates that the activity increase arose principally at the upper and lower borders of the field, with declining activity in midfield. That activity decline then spreads to occupy nearly the entire field, except for a small area on the top border of the image. The same regions behaved differently during QS and REM, with a later, and very widespread, activity increase in both states to the depressor challenge. Detailed descriptions of regional trends within the VMS were beyond the scope of this study; however, the regional patterns demonstrate that, within the overall averaged response, cellular groups can show unique trends.

DISCUSSION

Overview. Contrary to initial expectations, lowering of blood pressure during REM sleep activated the VMS substantially more than depressor challenges in waking or QS. Transient blood pressure elevation momentarily reduced activity on both the rostral and interme-

diolate areas of the VMS in waking and REM sleep, but the initial decline occurred only in rostral sites in QS. The initial declines to pressor challenges were followed by an activity increase in all states, and the rise was substantial. The VMS activity and blood pressure responses occurred on a background of diminished spontaneous activity on the VMS during REM sleep.

Cell groups. The probe sampled activity to a depth of 500 μm and from the exit of the Vth nerve caudally through the intermediate area. Although functional properties of the VMS have long been the object of attention, description of neurons on the surface has only recently been addressed; the focus instead has been on defined cell groups, such as those of the rostral ventrolateral medulla (RVLM) that project to the intermediolateral sympathetic cell column of the spinal cord. We speculate that the signals observed from the optical probes represent activity from anecdotally described small neurons on the VMS, together with

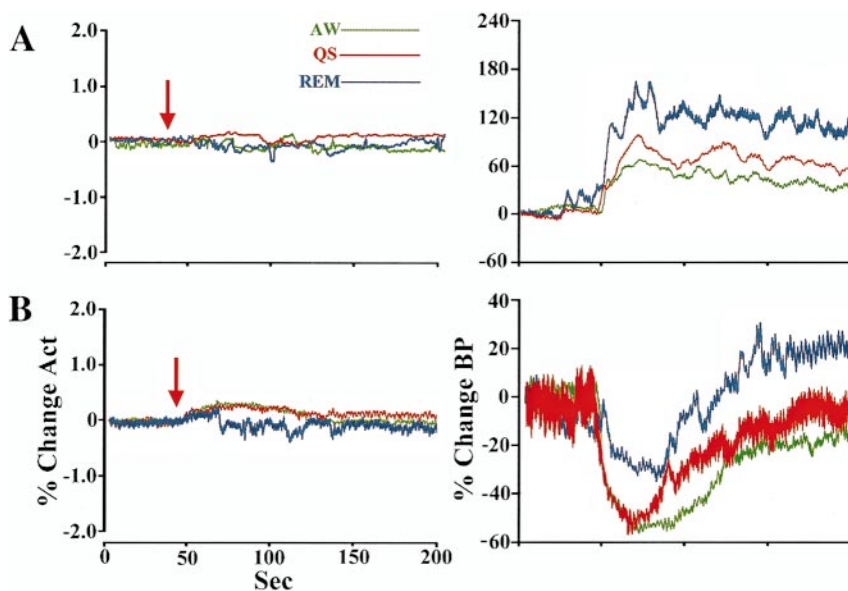


Fig. 7. Averaged activity traces (%Change Act) from a spinomedullary control site, together with blood pressure responses (%Change BP) accompanying phenylephrine (A) and nitroprusside (B) challenges. Challenge began at arrow in each condition.

dendritic activity from those cells, and that the evidence from the pressor and depressor challenges indicates a “compensatory” or modulating role of these cells on RVLM neurons.

Relationships to anesthetic state findings. Earlier data from the barbiturate-anesthetized cat preparation indicate a topographic organization of VMS responses to pressor and depressor challenges. Under barbiturate anesthesia, rostral VMS sites activate, with caudal areas also showing a decline in activity to depressor challenges, whereas both rostral and caudal regions show a decline to pressor challenges (10). Data from another species, the goat, indicate that rostral VMS activity rises during a depressor challenge in waking but increases more modestly during halothane anesthesia (11). Alternative means to lower blood pressure also increase VMS activity; substantial hypotension associated with hypovolemia elevates VMS activity, albeit after an initial activity decline during the sympathoexcitatory stage of the shock response (12). It appears that a depressor challenge activates the VMS and, under conditions of anesthesia, that activation may be confined to rostral regions. In addition, VMS activation may be more muted during anesthesia than during waking and sleep states can enhance the VMS response.

The time course of the VMS response to a pressor challenge during anesthesia (10) consists of two components, an initial rapid (30–60 s) activity decline followed by a slower (3–4 min) decline. Both components depend on the integrity of carotid sinus and vagal nerves; transection of the carotid sinus nerve enhances both components, whereas vagotomy nearly abolishes both aspects. In the drug-free animals used in the current study, activity rose after the initial decline. The data collected under anesthesia suggest that the nucleus of the solitary tract, which receives carotid sinus nerve input and relays information to the VMS, exerts a disfacilitatory or inhibitory influence on the VMS and an excitatory influence from the vagus to the pressor challenge. We speculate that the late-developing elevation in activity during waking and sleep states to pressor challenges could derive from interactions of VMS interneurons with peripheral afferent input; this input might be diminished with anesthesia.

Responses to pressor challenges. The initial response to a rise in blood pressure was an activity decline on the VMS. This decline was common to all sleep states and was reminiscent of activity changes described in earlier studies of anesthetized preparations (10, 11). The initial decline in activity was confined to the rostral VMS in QS that possibly reflects the reduced blood pressure rise to the phenylephrine challenges administered within the QS state (Fig. 4).

The state-related differences in the initial decline and subsequent rise in activity may depend on interactions between baroreceptor afferent activity from both carotid sinus and vagal sources that may exert influences at different times in the blood pressure response. The initial decline in activity may also result from a compensatory reaction to the baroreceptor loading

emerging from the smooth muscle contraction elicited by phenylephrine. Resolution of the source of influence and timing relationships will require blockade of vagal and carotid sinus nerve fibers during challenges within each state.

Responses to depressor challenges during REM sleep. Activity on the VMS to depressor challenges was maximal during the REM state. The extreme response during the REM state occurred despite the substantial decline in “spontaneous” VMS activity during REM sleep (29). The reduction in “spontaneous” VMS activity during REM sleep is unlike that which occurs in most brain areas, e.g., cortical, thalamic, or hippocampal sites, which show extensive activation during that state. However, isolated regions, including the dorsal raphe (18), raphe obscurus, and locus ceruleus (30), all areas that mediate aspects of blood pressure control, show a similar decline in activity during the REM state. The diminished VMS baseline activity during the REM state could result from loss of excitation or disfacilitation from other neural structures. That possibility is supported by the relative absence of influence from electrical or thermal stimulation of diencephalic structures on physiological processes during the REM state (5, 21, 23, 24).

The enhanced rise in VMS activity to a depressor challenge during REM sleep was unexpected. The overall decline in spontaneous activity on the VMS suggests a condition in which the region is unresponsive to external challenge; instead, the response was one that appeared to be of an unmodulated overactivation during the REM state. During waking and QS, the VMS activation was much more modest, as if the region were more closely regulated during these two states. The activity responses to blood pressure manipulation suggest that state-related external neural influences on the VMS act to dampen baroreflexes and that the VMS is “released” from such influences during REM sleep, especially during depressor challenges.

The “release from modulation” possibility could account for a portion of the physiological characteristics of REM sleep. The characteristics of enhanced respiratory and heart rate variability, different distribution of blood flow, and phasic enhancement of movements, breathing, and blood pressure could be viewed as a loss of control from normal-modulating structures during the REM sleep state. The significantly increased variability in both the cardiovascular system and respiratory musculature during REM sleep is suggestive of reduced control of output to autonomic and respiratory motor systems from one or more excitatory circuits. The VMS may play such a role in modulation of blood pressure.

VMS activity is restored toward baseline levels during both pressor and depressor challenges by phasic events within REM sleep. The phasic restoration of baseline activity may play an essential component in compensatory efforts to restore blood pressure from a hypotensive challenge. The source(s) of these periods of activation are currently being examined, but apparently involve the medial and descending vestibular

nuclei (20) and caudal-lateral regions of the pons (3). The overall contributions of vestibular systems to sympathetic outflow are well described (32). However, the means by which vestibular and pontine influences interact with VMS areas during the phasic events of REM sleep are not yet known.

Control responses. Pressor and depressor challenges elicited much smaller changes on control sites from those observed with VMS placements. Traces from a spinomedullary site, caudal to the XIIth nerve exit, and shown in Fig. 7, demonstrate minimal changes in the optical traces relative to the VMS sites, particularly at the onset of the response. Small signal changes occur later in the response, most likely associated with arousal components associated with the challenge. The responses from control sites indicate unique roles for the VMS in regulation of blood pressure, rather than a generalized property of neural tissue to respond to pressor or depressor manipulations.

Regional patterns. The regional patterns that emerged during the challenges between different states suggest that the collection of neurons that respond to the challenges interact differently from one state to another. Although a thorough description of the trends in regional patterns was beyond the scope of this study, the findings suggest a topographical organization of responses that differ between pressor and depressor challenges between waking and sleep states and may assist in determination of localized VMS neural responses to state-related blood pressure manipulations.

Clinical implications. The potential for VMS dysfunction or release from control during the REM state has significant implications for the sudden infant death syndrome (SIDS). The fatal event in SIDS is, at least in some instances, accompanied by bradycardia and loss of blood pressure (19). A possibility exists that the final event results from an uncompensated loss of blood pressure during sleep (9). A proportion of victims of SIDS shows diminished muscarinic binding in VMS regions that project to the caudal medullary structures mediating responses to hypotension (2, 13, 33). Although the mechanism(s) of failure in SIDS remains unclear, infants appear to succumb during sleep, and the fatal event may involve an inability to compensate for profound blood pressure loss, superimposed on diminished spontaneous activity of a structure, the VMS, which is already disfacilitated during REM sleep. Deficient cells on the VMS that cannot elicit appropriate responses to blood pressure challenges may participate in the fatal event.

In conclusion, the initial VMS responses to blood pressure elevation and lowering are reciprocal; pressor challenges result in an early decline in activity, and depressor challenges excite this region. The VMS responses to blood pressure manipulation suggest a "compensatory" role to restore normative levels of cardiovascular tone. The relative importance of this compensatory role varies with sleep states. During waking, the VMS plays a relatively unimportant role, especially for depressor challenges, but in the REM sleep state, during which forebrain structures exert little influence over

brain stem regions, the VMS responds remarkably to blood pressure challenges. Earlier, we found that wakefulness nearly abolished a pressor-induced activity decline found in the goat rostral VMS during anesthesia. Wakefulness apparently recruits brain regions other than the VMS to mediate a response to a pressor challenge. The data from blood pressure challenges during QS and REM sleep reinforce the concept that multiple brain sites exert state-dependent influences on the VMS and that, during REM sleep, these influences might be lost, leaving undampened VMS responses to challenges.

We thank Lisa Stallings and Rebecca Harper for technical assistance.

This research was supported by National Heart, Lung, and Blood Institute Grant HL-22418.

Address for reprint requests and other correspondence: R. M. Harper, Dept. of Neurobiology, Univ. of California at Los Angeles, Los Angeles, CA 90095-1763 (E-mail: rharper@ucla.edu).

Received 1 July 1999; accepted in final form 27 October 1999.

REFERENCES

1. **Cohen LB.** Changes in neuron structure during action potential propagation and synaptic transmission. *Physiol Rev* 53: 373–418, 1973.
2. **Coleman MJ and Dampney RA.** Powerful depressor and sympathoinhibitory effects evoked from neurons in the caudal raphe pallidus and obscurus. *Am J Physiol Regulatory Integrative Comp Physiol* 268: R1295–R1302, 1995.
3. **Datta S.** Cellular basis of pontine ponto-geniculo-occipital wave generation and modulation. *Cell Mol Neurobiol* 17: 341–365, 1997.
4. **Fitzgerald RS.** The regulation of breathing. In: *A History of Breathing Physiology. Lung Biology in Health and Disease*, edited by Proctor DF. New York: Dekker, 1995, vol. 83, p. 303–342.
5. **Frysinger RC, Marks JD, Trelease RB, Schechtman VL, and Harper RM.** Sleep states attenuate the pressor response to central amygdala stimulation. *Exp Neurol* 83: 604–617, 1984.
6. **Gozal D, Ohtake PJ, Rector DM, Lowry TF, Pan LG, Forster HV, and Harper RM.** Rostral ventral medullary surface activity during hypercapnic challenges in awake and anesthetized goats. *Neurosci Lett* 192: 89–92, 1995.
7. **Guertzenstein PG and Silver A.** Fall in blood pressure produced from discrete regions of the ventral surface of the medulla by glycine and lesions. *J Physiol (Lond)* 242: 489–503, 1974.
8. **Haglund MM, Hochman DW, Meno JR, Ngai AG, and Winn HR.** Mechanisms underlying the intrinsic signal during optical imaging of rat somatosensory cortex. *Soc Neurosci Abstr* 20: 1264, 1994.
9. **Harper RM and Bandler R.** Finding the failure mechanism in the Sudden Infant Death Syndrome. *Nat Med* 4: 157–158, 1998.
10. **Harper RM, Gozal D, Dong X-W, and Rector DM.** Pressor-induced responses of the cat ventral medullary surface. *Am J Physiol Regulatory Integrative Comp Physiol* 268: R324–R333, 1995.
11. **Harper RM, Gozal D, Forster HV, Ohtake PJ, Pan LG, Lowry TF, and Rector DM.** Imaging of VMS activity during blood pressure challenges in awake and anesthetized goats. *Am J Physiol Regulatory Integrative Comp Physiol* 270: R182–R191, 1996.
12. **Harper RM, Richard CA, and Rector DM.** Physiological and ventral medullary surface activity during hypovolemia. *Neuroscience* 94: 579–586, 1999.
13. **Kinney HC, Filiano JJ, Sleeper LA, Mandell F, Valdes-Dapena M, and White WF.** Decreased muscarinic receptor binding in the arcuate nucleus in sudden infant death syndrome. *Science* 269: 1446–1450, 1995.
14. **Li A, Randall M, and Nattie EE.** CO₂ microdialysis in the retrotrapezoid nucleus of the rat increases breathing in waking but not in sleep. *J Appl Physiol* 87: 910–919, 1999.

15. **Loeschke HH, DeLattre J, Schläpke ME, and Trouth CO.** Effects on respiration and circulation of electrically stimulating the ventral surface of the medulla oblongata. *Respir Physiol* 10: 179–184, 1970.
16. **Malonek D, Dirnagl U, Lindauer K, Yamada I, Kanno I, and Grinvald A.** Vascular imprints of neuronal activity: relationships between the dynamics of cortical blood flow, oxygenation, and volume changes following sensory stimulation. *Proc Natl Acad Sci USA* 94: 14826–14831, 1997.
17. **Mancia G, Baccelli G, Adams DB, and Zanchetti A.** Vasomotor regulation during sleep in the cat. *Am J Physiol* 220: 1086–1093, 1971.
18. **McGinty DJ and Harper RM.** Dorsal raphe neurons: depression of firing during sleep in cats. *Brain Res* 101: 569–575, 1976.
19. **Meny RG, Carroll JL, Carbone MT, and Kelly DH.** Cardiorespiratory recordings from infants dying suddenly and unexpectedly at home. *Pediatrics* 93: 43–49, 1994.
20. **Morrison AR and Pompeiano O.** Vestibular influences during sleep. *Arch Ital Biol* 108: 154–180, 1970.
21. **Ni H, Schechtman VL, Zhang J-X, Glotzbach SF, and Harper RM.** Respiratory responses to preoptic/anterior hypothalamic warming during sleep in kittens. *Reprod Fertil Dev* 8: 79–86, 1996.
22. **Ohtake P, Foster HV, Pan LG, Lowry TF, Korducki MJ, and Whaley AA.** Cardiovascular responses to cooling the ventrolateral medulla (VLM) in awake and anesthetized adult goats. *Soc Neurosci Abstr* 20: 843, 1994.
23. **Parmeggiani PL, Azzaroni A, Cevolani D, and Ferrari G.** Responses of anterior hypothalamic-preoptic neurons to direct thermal stimulation during wakefulness and sleep. *Brain Res* 269: 382–385, 1983.
24. **Parmeggiani PL, Franzini C, and Lenzi P.** Respiratory frequency as a function of preoptic temperature during sleep. *Brain Res* 111: 253–260, 1976.
25. **Phillipson EA, Sullivan CE, Read DJC, Murphy E, and Kozar LF.** Ventilatory and waking responses to hypoxia in sleeping dogs. *J Appl Physiol* 44: 512–520, 1978.
26. **Poe GR, Nitz DA, Rector DM, Kristensen MP, and Harper RM.** Concurrent reflectance imaging and microdialysis in the freely behaving cat. *J Neurosci Methods* 65: 143–149, 1996.
27. **Rector DM, Gozal D, Forster HV, Ohtake PJ, and Harper RM.** Ventral medullary surface activity during sleep, waking, and anesthetic states in the goat. *Am J Physiol Regulatory Integrative Comp Physiol* 267: R1154–R1160, 1994.
28. **Rector DM, Poe GR, and Harper RM.** A miniature CCD video camera for high-sensitivity measurements in freely behaving animals. *J Neurosci Methods* 78: 85–89, 1997.
29. **Richard CA, Rector DM, Harper RK, and Harper RM.** Optical imaging of the ventral medullary surface across sleep-wake states. *Am J Physiol Regulatory Integrative Comp Physiol* 277: R1239–R1245, 1999.
30. **Sakai K.** Executive mechanisms of paradoxical sleep. *Arch Ital Biol* 126: 239–257, 1988.
31. **Ursin R and Serman MB.** *A Manual for Standardized Scoring of Sleep and Waking States in the Adult Cat.* Los Angeles: Brain Information Service/Brain Research Institute, University of California, 1981.
32. **Yates BJ.** Vestibular influences on the autonomic nervous system. New directions in vestibular research. *Ann NY Acad Sci* 781: 458–470, 1996.
33. **Zec N, Filiano JJ, and Kinney HC.** Anatomic relationships of the human arcuate nucleus of the medulla: a DiI-labeling study. *J Neuropathol Exp Neurol* 56: 509–522, 1997.

